New phase-transfer decay mechanism for persistent currents in ^{3}He-A

Chia-Ren Hu
Department of Physics, Texas A&M University, College Station, Texas 77843
(Received 30 May 1978; revised manuscript received 27 April 1979)

When a magnetic field $\vec{B}$ prevents the orbital axis $\hat{l}$ from lining up with $\pm\vec{B}$ (in the dipole-locking regime), persistent-current states in superfluid ^{3}He-A are characterized by two quantum numbers n_w and n_t. These states can decay via two new phase-transfer mechanisms by which $n_w \pm n_t$ changes by multiples of 2, keeping $n_w \mp n_t$ constant. Intricate effects due to the presence of surfaces are analyzed. With modifications, the present analysis can also be applied to the zero-field case. Most useful conclusions are obtained in the helical-texture regime, and in a metastable situation with $\hat{l}$ locked in opposite directions on two parallel walls.

The purpose of this paper is to propose a new mechanism, which I named "phase transfer", for the decay of persistent currents in the A phase of superfluid ^{3}He, in wide channels and in the presence of a sufficiently strong magnetic field. This new mechanism is a generalization of the well-known concept of phase slip[1] to a superfluid whose order parameter is characterized by two or more independent phases, and refers in general to the notion of a simultaneous slippage of two or more phases under one or more constraints among them. Apparently the only clearly applicable system of this mechanism discovered to date is superfluid ^{3}He-A in wide channels (so that the spin axis $\hat{d}$ and the orbital axis $\hat{l}$ are locked in the same direction by the dipole interaction), and in the presence of a sufficiently strong magnetic field $\vec{B}$ (so that $\hat{d}$, and therefore $\hat{l}$, are prevented from lining up with $\pm\vec{B}$ at equilibrium). In such a case it is deduced here that the order parameter is characterized by two independent phases S_1 and S_2, and that there are two types of phase transfer, corresponding to the simultaneous slippage of S_1 and S_2, by $2\pi(\Delta n)$ and $\pm 2\pi(\Delta n)$, respectively, (where $\Delta n = \pm 1, \pm 2$, etc.), so that $S_1 \mp S_2$ remains "unslipped" (i.e., obeying the original quantization condition).

Below we first review the main features of the phase-slip mechanism in order to reveal a parallelism between the topological reasonings with which the phase-slip and the phase-transfer mechanisms are deduced.

For the present purpose, all *one-phase* superfluids, such as ^{4}He, all (s-wave-pairing) superconductors, and even ^{3}He-B, may be regarded as characterized by a complex scalar order parameter $\psi = f\exp(i\Phi)$. Such a system ensures a maximum gain in condensation energy by having $f = f_0$ (the equilibrium value), but it is degenerate with respect to Φ. The order-parameter-degeneracy (OPD) space[2,3] is therefore a circle S^1 in the complex ψ plane of radius f_0, centered at origin. Prescribing a continuous and single-valued order-parameter distribution on a closed curve Γ in a superfluid channel corresponds to a continuous mapping of Γ into S^1, which is obviously characterized by a topologically invariant winding number $n = 0, \pm 1, \pm 2$, etc. The value of n must be common to the whole set $\{\Gamma\}$ of all Γ's which are continuously deformable into each other without leaving the superfluid channel, and clearly $n \neq 0$ only for those $\{\Gamma\}$ whose members do not include a single point (as the limit of a small loop). Such a $\{\Gamma\}$ exists only in a multiply-connected channel; the resulting $n \neq 0$ states in such a channel are then the metastable persistent-current states of the superfluid.

The winding number n can change, and therefore the persistent current can decay, only by reducing some of the winding loops to points, without breaking the continuity of the mapping. In doing so the image of Γ must move into the region with $f < f_0$, where there is a condensation energy hill. To discuss such a process, the definition of n must be generalized to mappings not confined to S^1

$$n \equiv (2\pi)^{-1} \oint_\Gamma \vec{\nabla}\Phi \cdot d\vec{\Gamma} \ , \tag{1}$$

which is usually called the circulation quantum number, because $\vec{\nabla}\Phi$ is proportional to the superfluid velocity $\vec{v}_s$. Since Φ *is ill-defined only when* $f = 0$, Eq. (1) implies that n can change by $\Delta n (= \pm 1, \pm 2, \text{etc.})$ on a Γ, when and only when a loop in the image of Γ passes through the origin of the complex ψ plane, corresponding to f evolving to the value zero at one point on Γ. The phase Φ can then "slip" by $(2\pi)\Delta n$ there, *before* f resumes a nonvanishing value, while the mapping remains a continuous one all the time.

In order for the same phase slip to occur on all members of a set $\{\Gamma\}$, either of two possibilities must occur: In very thin channels, f can vanish on a whole surface σ whose boundary must enclose all members of $\{\Gamma\}$, thus creating what is now known as a phase-slip center. The region where $f \neq f_0$ must be localized on both sides of σ on energetic ground.

For channels that are large at least in one dimension perpendicular to the persistent currents (henceforth, called wide channels), it is energetically too costly to create a phase-slip center. Instead, it is only necessary for f to vanish on a single curve γ, if only this γ will move and sweep a whole surface σ as defined above, thus allowing the same phase slip to occur on all members of $\{\Gamma\}$, albeit not all at the same time. In order to achieve this, the curve γ must divide the imaginative surface σ into two parts σ_1 and σ_2, so that the integral $(2\pi)^{-1}\oint_\Gamma \vec{\nabla}\Phi\cdot d\vec{r}$ can take the value n if $\Gamma=\Gamma_1$, which passes through σ_1 once, and not through σ_2; while the same integral can take the value $n-\Delta n$ if $\Gamma=\Gamma_2$, which passes through σ_2 once, and not through σ_1. As γ moves so that σ_2 grows from a null set to the whole σ, the circulation quantum number then changes from n to $n-\Delta n$. Clearly γ is characterized by a quantization condition

$$(2\pi)^{-1}\oint \vec{\nabla}\Phi\cdot d\vec{r}=\Delta n \ , \qquad (2)$$

where the integration path is any closed path encircling γ in a direction so that it is topologically equivalent to tracing Γ_1 in the forward direction, followed by tracing Γ_2 in the backward direction. Two possibilities still exist for the curve γ. It may end on the boundary (or boundaries) of σ, or form a closed loop. The corresponding entities have been known as a vortex line and a vortex ring, respectively, and the process as vortex flow (or flux-flow in the superconductivity literature).

We are now ready to show that a generalization of the above analysis can apply to ^{3}He-A under the conditions specified, if the condition $f=0$ is replaced by two possible conditions $\cos\chi=\pm1$, leading to the two types of phase transfer mentioned in the introduction.

The pair-wave-function order-parameter of ^{3}He-A has an orbital part in the form $\Delta_0(\hat{m}+i\hat{n})\cdot\hat{k}$,[4] where $\hat{m}\perp\hat{n}$ are two unit vectors with $\hat{l}=\hat{m}\times\hat{n}$, and $\hat{k}$ denotes the relative momentum vector of the pairs normalized to unit length. The spin part is suppressed here since the assumption of dipole locking leaves no extra degrees of freedom in the spin space. The system is degenerate with respect to the choice of the triad $(\hat{m},\hat{n},\hat{l})$, which may always be obtained from a reference triad $(\hat{x},\hat{y},\hat{z})$ by a rotation about an axis of polar angles (θ,ϕ) by an angle $r\pi$ (where $0<r<1$). The OPD space [i.e., the collection of all (r,θ,ϕ)] is therefore represented by a solid sphere of unit radius with its antipodal boundary points identified, which in topology is called the three-dimensional projective space P_3 (cf, Fig. 1).[2,3] As shown in Refs. 2 and 3, a closed space curve Γ can only be mapped into P_3 in two topologically distinct classes—those with images topologically equivalent to a point and a diameter, respectively. This explains why persistent currents in ^{3}He-A in the absence of an external magnetic field must rely on the bending energy to stabilize itself and be barely stable under suitable conditions only (on temperature, channel width, etc.).[5]

The situation is different when a magnetic field $\vec{B}$ is applied. If the dipole locking is perfectly effective and the field $\vec{B}$ is very strong, the orbital axis $\hat{l}$ must lie perpendicular to $\vec{B}$. The OPD space becomes $S^1\times S^1$, whose fundamental homotopy group is $Z\times Z$, where Z is the set of integers.[6] (See also Fig. 1.) Persistent currents can therefore exist and are characterized by two integers.[6] Actually the condition may be relaxed somewhat. The magnetic field need only be so strong, and the dipole locking so effective, as to prevent $\hat{l}$ from lining up with $\pm\vec{B}$ at any equilibrium or steady states; then persistent currents can already exist, and are still characterized by two quantum numbers n_2 and n_l, as defined below.

In P_3 the equations $\hat{l}\parallel\pm\vec{B}$ correspond to the polar

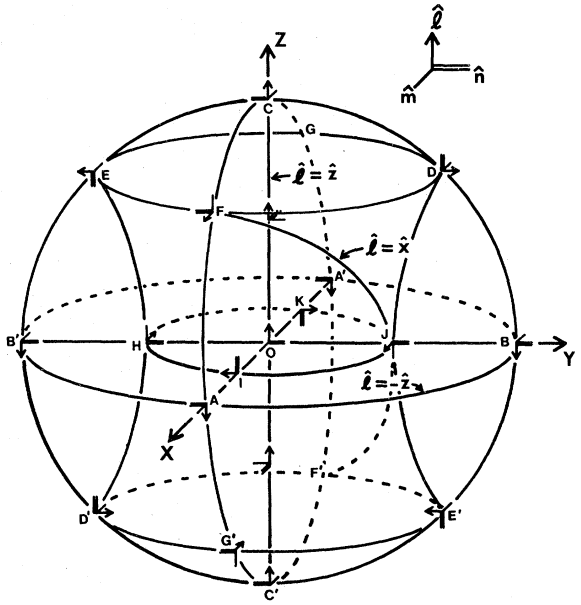

FIG. 1. Order-parameter-degeneracy space of ^{3}He-A is the three-dimensional projective space P_3, represented by a solid sphere with its antipodal boundary points identified. (e.g., A' with A, B' with B, etc.) A point of polar representation (r,θ,ϕ) in this space, with $r\leq1$, corresponds to a rotation about (θ,ϕ) by $r\pi$, which acts upon the triad $(\hat{x},\hat{y},\hat{z})$ to give a possible orientation of the triad $(\hat{m},\hat{n},\hat{l})$. Thus the polar diameter corresponds to $\hat{l}=\hat{z}$. The equator, $\hat{l}=-\hat{z}$. A curve connecting F, J, and F' corresponds to $\hat{l}=\hat{x}$. The surface of revolution generated by rotating the $\hat{l}=\hat{x}$ curve about $\hat{z}$ corresponds to the condition $\hat{l}\perp\hat{z}$, and becomes the order-parameter-degeneracy space of ^{3}He-A in the presence of a very large magnetic field in the dipole-locking regime. This is the hour-glass-shaped surface connecting the circles $EFDG$, $HIJK$ and $E'F'D'G'$. It has the topology of a torus (i.e., $S^1\times S^1$), after realizing the identification of $EFDG$ and $E'F'D'G'$.

diameter and the equator, respectively, after choosing $\hat{z}$ and the polar axis of P_3 to be along $\vec{B}$. It is then important to realize that both the polar diameter and any semicircle on the equator are *closed interior* curves of P_3, thanks to the identification of antipodal boundary points. With neighborhoods of these curves as forbidden zones, a mapping of Γ is clearly now characterized by two independent winding numbers. Referring to Fig. 1, we anticipate later need and define a winding around the polar diameter as positive if it is topologically equivalent to the closed curve *HIJK*. On the other hand, a winding around the equator is positive if it is topologically equivalent to the *closed* curve $EHD'(=D)JE'(=E)$. These two winding numbers can still be both integers *or both half odd integers,* with the latter case corresponding to mappings with images starting and ending on the two identified antipodal boundary points of P_3 (e.g., a curve connecting $E'IE$ in Fig. 1 is equivalent to $E'G'D'HE$, or $E'JDFE$, or $D'F'E'JD$). We therefore define these winding numbers as $\frac{1}{2}(n_w \mp n_t)$, respectively [i.e., with (+) sign for winding around the equator], so that n_w and n_t can only take *arbitrary* integer values. To give a more useful definition for n_w and n_t, as Eq. (1) is for n, we turn to the following representation for the order parameter which is recently employed by Tsuneto *et al.*[7]:

$$\hat{m}+i\,\hat{n}=A_+\frac{\hat{x}+i\,\hat{y}}{\sqrt{2}}+A_-\frac{\hat{x}-i\,\hat{y}}{\sqrt{2}}+A_0\hat{z}\ ,$$
$$A_\pm=\pm(1/\sqrt{2})(1\pm\cos\chi)\exp[i(S_1\pm S_2)]\ , \qquad (3)$$
$$A_0=\sin\chi\exp(iS_1)\ .$$

Note that S_1 is the overall phase, while $2S_2$ stands for the relative phase between the $\pm(\hat{x}\pm i\,\hat{y})\cdot\hat{k}\propto -Y_{1,\pm1}(\hat{k})$ components of the pair wave function. The phase of the $\hat{z}\cdot\hat{k}\propto Y_{1,0}(\hat{k})$ component is then fixed by the conditions $\hat{m}^2=\hat{n}^2, \hat{m}\cdot\hat{n}=0$, which are equivalent to $2A_+A_-=-A_0^2$, indicating that there are only two independent phases in the present situation. (The variable χ is not phase-like since it must satisfy $0<\chi<\pi$ for an equilibrium or steady state.) Note also that under the restrictions $0<\chi<\pi$, $0<S_1,\ S_2<2\pi$, the variables (S_2,χ,S_1) are just one definition of the Euler angles, as illustrated in Fig. 2. Thus, it follows from Eq. (3) *or* Fig. 2 that

$$\hat{m}=\cos S_1\hat{p}-\sin S_1\hat{q},\quad \hat{n}=\sin S_1\hat{p}+\cos S_1\hat{q}\ , \qquad (4a)$$

where

$$\hat{p}=\cos\chi(\cos S_2\hat{x}-\sin S_2\hat{y})+\sin\chi\,\hat{z}\ ,$$
$$\hat{q}=\sin S_2\hat{x}+\cos S_2\hat{y}\ ,$$

and

$$\hat{l}=-\sin\chi\cos S_2\hat{x}+\sin\chi\sin S_2\hat{y}+\cos\chi\,\hat{z}\ . \qquad (4b)$$

However, it is more convenient here to let $S_{1,2}$ be unrestricted, like Φ is treated for a one-phase superfluid. At equilibrium, $\sin\chi\neq 0$ and $\cos\chi\neq\pm1$. Then requiring $\hat{m}+i\,\hat{n}$ to be single valued and continuous on a closed curve Γ immediately leads to the following quantization conditions:

$$n_w=(2\pi)^{-1}\int_\Gamma \vec{\nabla}S_1\cdot d\vec{r}\ ,$$
$$n_t=(2\pi)^{-1}\int_\Gamma \vec{\nabla}S_2\cdot d\vec{r}\ . \qquad (5)$$

That this definition agrees with the previous one can be verified by considering the result of continuously reducing χ to 0 or π, which does not change the winding number around the equator or the polar diameter, respectively: As the limit $\chi\to 0$ is taken, $\hat{l}\to\hat{z}$, S_1+S_2 becomes the only meaningful phase, which advances by $2\pi(n_w+n_t)$ as Γ is traced. This corresponds to the winding of $\hat{m}$ and $\hat{n}$ about $\hat{l}=\hat{z}$ by $-(n_w+n_t)$ turns in the right-handed sense. The curve γ must therefore have been mapped onto $C0C'$ of Fig. 1 n_w+n_t times, corresponding to winding around the equator $\frac{1}{2}(n_w+n_t)$ times in the sense defined before. Similarly, as the limit $\chi\to\pi$ is taken, $\hat{l}\to\hat{z}$, S_1-S_2 becomes the only meaningful phase, which advances by $2\pi(n_w-n_t)$ as Γ is traced. This corresponds to the winding of $\hat{m}$ and $\hat{n}$ about $\hat{l}=-\hat{z}$

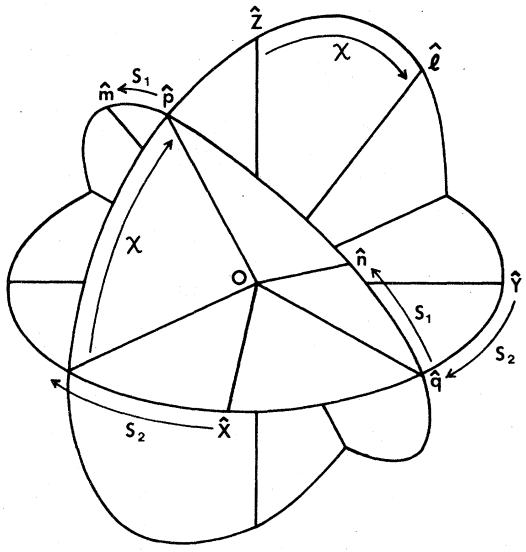

FIG. 2. Variables (S_2,χ,S_1), introduced in Eq. (3) for describing the orientation of the triad $(\hat{m},\hat{n},\hat{l})$, may be understood as an alternative definition for the Euler angles: The triad $(\hat{m},\hat{n},\hat{l})$ are obtained from the reference triad $(\hat{x},\hat{y},\hat{z})$ by three consecutive rotations, namely, first a rotation about the z axis by $-S_2$, then followed by a rotation about the new y (i.e., $\hat{q}$) axis by $-\chi$, and finally followed by a rotation about the new z (i.e., $\hat{l}$) axis by $-S_1$.

by $-(n_w - n_t)$ turns in the right-handed sense. The curve Γ must therefore have been mapped onto $B'AB$ $n_w - n_t$ times, corresponding to winding around the polar diameter $\frac{1}{2}(n_w - n_t)$ times in the sense defined before.

We suggest calling n_w and n_t the winding and tumbling quantum numbers, because if only $n_w \neq 0$, $\hat{m}$ and $\hat{n}$ would wind around $-\hat{l}$ right handedly as Γ is traced, whereas if only $n_t \neq 0$, $\hat{l}_\perp$ $[\equiv \hat{l} - (\hat{l}\cdot\hat{z})\hat{z}]$ would tumble around $-\hat{z}$ right handedly as Γ is traced. (Note that $|\hat{l}_\perp|$ may vary along Γ, but it never vanishes to make the tumbling number ambiguous.) When both n_w and n_t are not equal to zero, the image of Γ in P_3 is a closed helix which simultaneously winds around the equator and the polar diameter by $\frac{1}{2}(n_w \pm n_t)$ times.

The most important point to realize from Eq. (3) now is that *$S_1 \pm S_2$ is ill-defined when and only when* $\cos\chi = \mp 1$, *i.e.*, *$\chi = \pi$ or 0*, and that for no value of χ are both S_1 and S_2 ill-defined at the same time. (This may also be seen readily from the Euler-angle interpretation given in Fig. 2.) Thus in order to change n_w and n_t without reducing Δ_0 to zero anywhere, it is necessary to have a simultaneous slip of S_1 by $2\pi(\Delta n)$, and of S_2 by $\pm 2\pi(\Delta n)$, where $\Delta n = \pm 1, \pm 2$, etc., at a point on Γ where χ evolves to the value π or 0, corresponding to the image of Γ cutting through the equator or the polar diameter, respectively. Then $n_w \pm n_t$ would change by $2\Delta n$, with $n_w \mp n_t$ kept unchanged. This is the two types of phase transfer mentioned in the introduction. Clearly, both types must be employed in order to change n_w and n_t independently.

Since $\chi = \pi$ or 0 corresponds to $\hat{l} \parallel \pm \vec{B}$, respectively, we shall call the corresponding types of phase transfer the A (antiparallel)-type and the P (parallel)-type respectively.

The ^{3}He-A channel under the conditions specified corresponds to the wide-channel limit as defined previously, because the assumption of dipole locking requires the channel width $W >> \xi_D \simeq 10^{-3}$ cm (the dipole characteristic length).[4] Thus in order for the same phase transfer to occur on all members of a set $\{\Gamma\}$, χ must take the value π or 0 on a curve γ which must then move to sweep a whole surface σ in much the same way that vortex flow takes place in a one-phase superfluid. Again the curve γ must either end on the surface of the channel, or form a closed loop. It is not difficult to see that the line case is related, but not identical, to the coreless vortex-line texture as introduced by Anderson and Toulouse[8]; while the ring case is related, but not identical, to a particle-like soliton as envisaged by Volovik and Mineev,[9] which may also be viewed as a coreless vortex ring texture,[9,10] since the line and ring here must each be made of two types: The A-type is characterized by an axis γ where $\chi = \pi$, $\hat{l} \parallel \hat{B}$, and the quantization condition

$$(2\pi)^{-1}\int \vec{\nabla} S_1 \cdot d\vec{r} = (2\pi)^{-1}\int \vec{\nabla} S_2 \cdot d\vec{r} = \Delta n \quad , \qquad (6)$$

whereas the P-type is characterized by an axis γ where $\chi = 0$, $\hat{l} \parallel \vec{B}$, and the quantization condition

$$(2\pi)^{-1}\int \vec{\nabla} S_1 \cdot d\vec{r} = -(2\pi)^{-1}\int \vec{\nabla} S_2 \cdot d\vec{r} = \Delta n \quad . \qquad (7)$$

In Eqs. (6) and (7), Δn and the integration path are defined in exactly the same way as those used in Eq. (2). Based on Eqs. (6) and (7), we note that the vortex line texture introduced here actually appears more like a Mermin–Ho texture,[11] rather than an Anderson–Toulouse texture,[8] especially if $\Delta n = 1$, and the texture axis is parallel to $\vec{B}$. This is particularly true if one disregards the far region, where the distance from the axis ρ is comparable with or larger than W, L/n_w, or L/n_t, with L denoting the length of the channel along the flow. (In this far region the vortex texture must distort itself to fit into the background texture.) In the region $\rho >> \xi_D$, the $\hat{l}$ vector must lie nearly perpendicular to $\vec{B}$, and rotate around $\vec{B}$ by $2\pi\Delta n$, when a full circle around and perpendicular to the axis γ is traversed. Thus unless $\Delta n = 1$ and the texture axis is parallel to $\vec{B}$, the texture cannot have cylindrical symmetry, even after the far region is disregarded. On the other hand, for a vortex ring texture with ring radius $a << W$, L/n_w, and L/n_t, the space around the ring texture is mapped into only one half of the four-dimensional-sphere representation of P_3 (defined by one sign of $\hat{l}\cdot\hat{z}$), rather than the full sphere as for the case of a Volovik–Mineev soliton.[9] The ring texture can not have cylindrical symmetry, for whatever orientation of $\vec{B}$ and the ring axis, since on the axial circle of the ring, $\hat{l} \parallel \pm \vec{B}$, while for $a << r << (WL/n_w$ and $L/n_t)$, $\hat{l}$ must be nearly perpendicular to $\vec{B}$ and must vary only in a general direction perpendicular to the ring. Thus the ring texture introduced here must appear rather different from those envisioned by Fujita *et al.*,[10] and depends strongly on the relative orientation of the ring and the applied field $\vec{B}$.

It should be noted also that a state (n_w, n_t) can only be changed to the $(n_w - n_A - n_P,\ n_t - n_A + n_P)$ states by the combined use of the two types of phase transfer, where n_A and n_P are arbitrary integers, corresponding to the effective numbers of A and P types of single-quantized $(\Delta n = 1)$ coreless vortex textures employed. Thus the $(\pm 1, 0)$ and $(0, \pm 1)$ states must decay to the (0,0) state via the usual phase-slip mechanism only, i.e., by the motion of usual vortex lines or rings with singular cores. In Fig. 3, we have conjectured the most likely decay paths for a number of initial states.

The energy required to create a coreless vortex texture of either type can be easily estimated. In a strong magnetic field, when the lateral dimension of

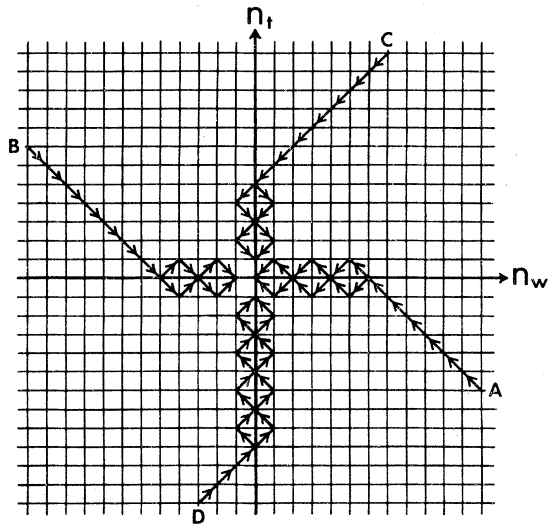

FIG. 3. Conjecture of most likely decay paths for a number of initial states of various n_w and n_t. Note that some initial states (A and B) employ purely P-type vortex textures for the initial decay, while some other initial states (C and D) employ purely A-type vortex textures for the same purpose; but toward the end there seems to be a degeneracy (or near degeneracy) in the choice of paths. Note also that states with odd $n_w \pm n_t$ can never reach the origin by phase-transfer processes only.

the texture is $\sim\xi_D$, it is of the order

$$g_D \xi_D^2 W \gtrsim 10^{-11}(1 - T/T_c) \text{ erg} , \tag{8}$$

where

$$g_D \simeq 10^{-3}(1 - T/T_c) \text{ erg/cm}^3$$

is the dipole energy density, and $W \gtrsim 10^{-2}$ cm is the typical width of the channel. At weaker fields both g_D and ξ_D must be replaced by a smaller g_H (the magnetic energy density) and a larger ξ_H (the magnetic characteristic length),[4] but the energy estimate remains the same. The thermal energy kT in the millikelvin range is of the order 10^{-19} erg, so thermal fluctuation can cause a rapid decay of n_w and n_t only for $1 - T/T_c \lesssim 10^{-8}$. The energy estimated in Eq. (8) is of the same order as a singular vortex line; the actual difference being in numerical coefficients and logarithmic factors not included in the present crude estimation.[12]

We now consider the effect of a plane boundary on the phase-transfer processes. If the boundary surface is perpendicular to the $\vec{B}$ field, then $\chi = \pi$ or 0 on the surface, which is therefore also classified into A- and P-types.[4] If an A-type coreless vortex line ends on a P-type surface (or vice versa), a surface point singularity named boojum[13] must clearly appear [see Fig. 4(a)]. In this case therefore, the motion of a boojum is not an independent decay mechanism for the persistent current, but is merely the necessary end configurature of the wrong type of coreless vortex textures, for that surface. For a P-type surface, on which only the combination $n_w + n_t$ is a meaningful quantum number, the combination changes when the same combination in the bulk changes, by the motion of an A-type coreless vortex texture. When a P-type vortex texture, which can end on a P-type surface without creating a surface singularity, moves to alter the $n_w - n_t$ combination in the bulk, it leaves the surface quantization conditon unaffected.

Next we consider a boundary surface oriented parallel to B, say perpendicular to the x axis. (The

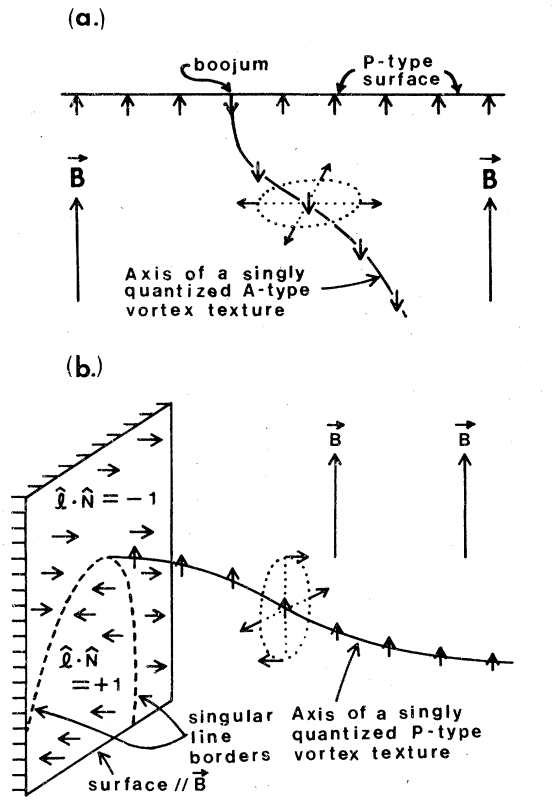

FIG. 4. (a) When a boundary surface is oriented perpendicular to the applied field $\vec{B}$, the surface may be classified as P-type, if $\hat{l} \parallel \vec{B}$ on this surface; or A-type, if $\hat{l} \parallel -\vec{B}$ on this surface. A boojum must then be created if an A-type vortex texture ends on a P-type surface, as shown. Same is true if A and P are interchanged. (b) When a boundary surface is oriented parallel to the applied field $\vec{B}$, then the axis of any coreless vortex texture must end on this surface at the tip of wedge-shaped regions of opposite $\hat{l} \cdot \hat{N}$ where $\hat{N}$ denotes the surface normal. (Only one wedge-shaped region is shown in the figure, corresponding to the case when the coreless vortex texture is singly quantized, i.e., with $\Delta n = 1$.) Each wedge-shaped region is separated from the rest of the surface by two singular line borders of ill-defined $\hat{l}$, which must cost large condensation energy to create.

current can still flow along any direction in the y-z plane.) Then on the surface $\chi=\frac{1}{2}\pi$, and $S_2=p\pi$, corresponding to $\hat{l}\cdot\hat{x}=(-1)^{p+1}$, where $p=0, \pm1, \pm2$, etc. To require a nonsingular texture in the bulk, an $n_t\neq0$ state must be accompanied by alternate surface regions of opposite $\hat{l}\cdot\hat{x}$, separated by borders[13] which must intersect with every path Γ confined on the surface. The total number of such surface regions must be $2n_t$. If an isolated coreless vortex line ends on such a surface, the end point must be the tip of wedge shaped regions on the surface with opposite $\hat{l}\cdot\hat{x}$, since the motion of such a texture changes n_t [see Fig. 4(b)]. As surface disgyration lines probably cost large condensation energy to create, we conjecture that a general state with $|n_w|>|n_t|$, $n_w n_t>0$, for example, would probably first employ only the A-type vortex textures to step down to the $(n_w-n_t,0)$ state. (If the starting state has $|n_w|>|n_t|$, $n_w n_t<0$, only P-type would be employed to reduce n_t to zero.) After that if the new n_w is still $\neq0$, then the system would employ *pairs* of *single*-quantized A and P types of vortex textures maintained at equilibrium distances, determined by balancing the bulk bending energy (which causes the A-P types to repel each other), and the surface border energy (which makes the A-P types attract each other). The later energy arises because the axes of the A-P pairs of vortex textures must end on the surface at the two tips of a mouth-shaped island[13] of opposite $\hat{l}\cdot\hat{x}$, bordered by two disgyration lines which must cost energy to form. Any Γ in the bulk, therefore, is predicted to quickly pass through the $n_t=\pm1$ states for the shortest possible duration allowed by energy considerations, for each reduction of 2 in $|n_w|$. (If the initial state has $|n_t|>|n_w|$, it can follow the decay paths depicted in Fig. 3 without ever increasing its $|n_t|$. Then this last consideration does not apply.) If a vortex ring is employed to change n_t, it must eventually grow so big as to lay a section of its axis on the surface. This line segment must then mark the appearance or disappearance of an area of opposite $\hat{l}\cdot\hat{x}$ on the surface. An $|n_t|$ increasing ring, after growing so big as to have created a mouth-shaped island on the surface, must slow down its growth, until another $|n_t|$ decreasing ring grows so big as to split the island into two. The two rings are then converted to two A-P pairs of opposite Δn, each attached to its own island on the surface, which can then move away from each other.

So far, only plane boundaries parallel or perpendicular to the $\vec{B}$ field have been considered. Generalizations to other orientations or even to curved surfaces seem to be a nontrivial task, and have not yet been worked out.

The phase-transfer mechanisms are developed here mainly for the case when the magnetic and dipole energies have provided energy barriers near $\chi=0$ and π, so that the situation is analogous to a one-phase superfluid which has a condensation energy hill near $f=0$. However, it is actually helpful to apply this line of thinking even in analyzing the decay of a persistent current in ^{3}He-A in the absence of an applied field (assuming that such states are locally stable which must still be verified, except in the wide-channel large-current limit, i.e., when $v_s W>>\hbar/2M$, which has already been studied[5,15]).

For concreteness let the channel have a slab geometry of width W with a flow in a direction parallel to the walls. Based on our present day knowledge, at least three regimes must be distinguished: As shown by the author in a separate paper,[14] if we characterize the flow by a parameter Q, representing an average phase gradient in the flow direction, then a critical value $Q_c\sim W^{-1}$ exists, such that for $Q<Q_c$ the $\hat{l}$ vector remains anchored normal to the walls. Applying Eq. (3) to this situation with z axis chosen perpendicular to the walls, we find $\chi=0$ (or π) in the equilibrium or steady states, with S_1+S_2 (or S_1-S_2) the only meaningful phase which becomes ill-defined when $\chi=\pi$ (or 0). Thus the flow is characterized by one quantum number n_w+n_t (or n_w-n_t), which decays via the motion of a modified version of A (or P) type of coreless vortex textures only.[15] Such a vortex texture must end on each wall with a boojum, and the resulting configuration is an Anderson–Toulouse vortex texture[8] as modified by Mermin,[13] studied also analytically in Ref. 12.

At Q_c, a textural transition has been predicted to occur,[14] which should be second order if $W>>\xi_D$, and first order if $W<<\xi_D$. Lacking sufficient information at the present time for the texture above Q_c in the case of $W<<\xi_D$, we confine our discussion here to the case $W>>\xi_D$. Then for $Q>Q_c$, the $\hat{l}$ vector deviates from normal to the walls in a nonplanar fashion, but retains a translational invariance parallel to the surfaces. Still applying Eq. (3) with z axis normal to the walls, we now have $\chi\neq0$ or π throughout the bulk region in a steady flow state. Thus the current carrying states must now be characterized by both quantum numbers n_w and n_t, but one expects that only $n_t=0$ states have a chance of being locally stable. Assuming that this is the case, which still needs to be verified, the decay of such $n_w\neq0$ states must invoke the motion of closely spaced A-P pairs of vortex-textures (original version, but in a different background texture) in order to quickly pass through an unstable $|n_t|=1$ state, in each reduction of $|n_w|$ by 2. The spacing between an A-P pair should now be comparable to the lateral dimension of the individual vortex textures (which is $\sim W$), forming a single entity which we might call a bound A-P pair. A closer look reveals that a bound A-P pair is nothing but an Anderson–Toulouse vortex texture as modified by Mermin to incorporate the boundary effects, but with the distortion due to the current further taken into account, as shown in Fig. 5.

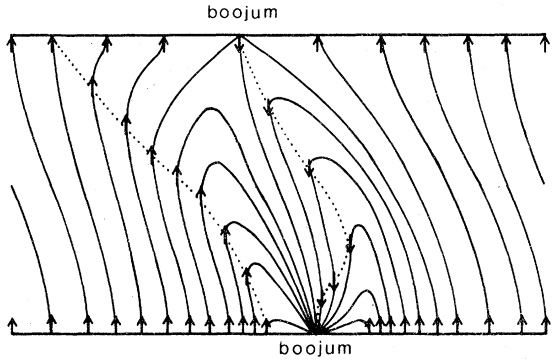

FIG. 5. Bound A-P pair as defined in the text is just an Anderson–Toulouse vortex texture as modified by Mermin to incorporate the boundary effects, but with the distortion due to the current further taken into account. Note the two lines with $\hat{l} = \pm \hat{z}$ stretching from one surface to the other. Note also that one such line must end on the two surfaces ($\perp \hat{z}$) as two boojums.

For $QW >> 1$, another regime can exist at proper conditions, where $\hat{l}$ spirals around the flow direction like a helix.[16] Since wall effects may be neglected in this case, it is more useful to apply Eq. (3) with the z axis chosen along the flow. Then again the current-carrying states are characterized by two quantum numbers n_w and n_t.[17] To discuss the decay of such a state, we first note that Eq. (3) implies that

$$\vec{V}_s = (\hbar/2M)(\vec{\nabla} S_1 + \cos\chi \vec{\nabla} S_2)$$
$$= (h/2ML)(n_w - \cos\theta_0 n_t) \ ,$$

where θ_0 is the constant apex angle of the helical texture,[15] and L is the length of the channel along the flow. Furthermore, $-2\pi n_t/L$ is just the parameter p introduced by Fetter,[16] properly quantized in a closed channel. [The minus sign arises from identifying his (θ, ϕ) as our $(-\chi, -S_2)$.] According to him, p must be near an optimum value p_{opt}, which is negative when V_s ($\propto$ Fetter's w) and $\cos\theta_0$ are positive. This implies that n_w and $n_t \cos\theta_0$ always have opposite signs, and according to Fig. 3, their decay should be principally via the P-type vortex texture only (assuming $\cos\theta_0 > 0$), although every some time an A-type vortex texture must be employed to keep p in the vicinity of p_{opt}. (In applying Fig. 3 to this case, the vicinity of the origin should be ignored, since the condition $QW >> 1$ will be violated long before that region is reached.) Since P here means parallel to the flow, the helical apex angle is locally reduced to zero at the axis of a P-type vortex texture, and to 180° at the axis of an A-type vortex texture. In most cases, the apex angle is not close to 90°, so there is no symmetry between $\chi = 0°$ and $\chi = 180°$. For the case when $\cos\theta_0 > 0$, an A-type vortex texture is expected to cost considerably more energy to create than a P-type one. In such a case, therefore, the current decay is expected to go through stages with pauses in between, so as to wait for an A-type vortex texture to be created. The case $\cos\theta_0 < 0$ may be discussed similarly, except that the roles played by A and P types of vortex textures must be interchanged.

There is yet another zero-field case which can be benefited by applying the present line of analysis. In a slab geometry before a current is introduced, the texture can also be locked in a metastable state with $\hat{l}$ pointing at opposite directions on the two surfaces. Then one can again apply Eq. (3) with z axis chosen normal to the boundary surfaces, finding $\chi \neq 0, \pi$ throughout the bulk region, so that a current carrying state with such boundary conditions must be again characterized by the two quantum numbers n_w and n_t. An important difference between this case and the situation discussed above for $Q \gtrsim Q_c$ is that for the present case, states with $n_t \neq 0$ can also be locally stable. The decay of an (n_w, n_t) state must also be via coreless vortices whose topological classification into A- and P-types is the same as before, but the appearances of these vortex textures are actually quite different, due to the different boundary conditions they must now satisfy (cf. Fig. 6). Furthermore, in the present case the two types of vortex textures will not

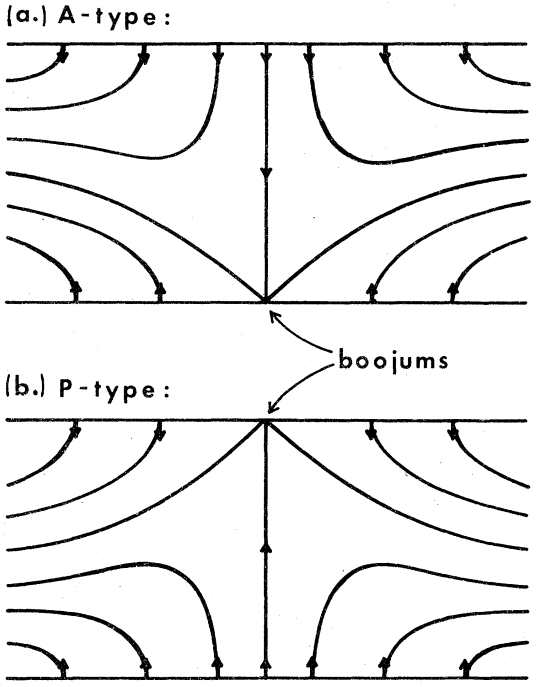

FIG. 6. Singly quantized A- and P-types of vortex textures in a situation when $\hat{l} \cdot \hat{N}$ has opposite signs on the two parallel walls and no magnetic field is applied. These textures have cylinder symmetry (before they are fit into a background texture of finite n_w and n_t). The $\hat{l}$ vectors need not be confined to the radial planes as shown, but are taken to be so just to give a simple illustration. Note that only one end of the axis of each texture creates a boojum on one of the two walls.

be expected to form "bound A-P pairs" in the sense discussed before. The two types of vortex textures should now cost essentially the same amount of energy for their creation, so the situation is in fact closest to the finite field case discussed in the earlier part of this work. In particular, Fig. 3 should also apply here in suggesting the most likely decay paths for various initial states.

In conclusion, we point out that the present work has provided us a new conceptual framework with which a quantitative theory can be developed for the decay of persistent currents in dipole-locked ^{3}He-A in a magnetic field. The theory will have a close analogy with that of vortex flow in superfluid ^{4}He or in superconductors, with corresponding roles played by f versus $\sin\chi$, Φ versus S_1 and S_2, singular vortex lines versus two types of coreless vortex textures, and the time-dependent Ginzburg-Landau (TDGL) equations (or their equivalent) versus the hydrodynamic equations (plus the effects of the dipole interaction and the magnetic field). We note that the TDGL equations must be derived microscopically because the magnitude of the order parameter f is not a hydrodynamic variable. The range of validity of these equations is therefore usually limited. Such a weakness does not exist for the ^{3}He-A system considered, because only hydrodynamic variables are involved (except possibly near the cores of point boojum singularities on the surface, which carry negligible weight in the theory). This is because hydrodynamic equations can be derived from purely phenomenological considerations, such as conservation laws and symmetry principles, leaving only a finite number of parameters to be determined by microscopic calculations, or by appealing to experiments. Such a set of hydrodynamic equations for ^{3}He-A has already been derived previously.[18] As to the zero-field case, we believe that the conceptual framework laid in this paper can also serve as a good starting point in constructing a quantitative theory for the decay of a persistent current, provided that a clear knowledge of the steady-state current-carrying states is available, and suitable adaptations are made (according to the circumstances) on the various definitions and concepts introduced here, as is exemplified in the previous four paragraphs.

This work was supported by the NSF under Grant No. DMR 76-81328.

---

[1]P. W. Anderson, Rev. Mod. Phys. 38, 298 (1966).

[2]G. Toulouse and K. Kleman, J. Phys. Lett. (Paris) 37, L-149 (1976).

[3]G. E. Volovik and V. P. Minneev, Pisma Zh. Eksp. Teor. Fiz. 24, 605 (1976), and Zh. Eksp. Teor. Fiz. 72, 2256 (1977).

[4]A. J. Leggett, Rev. Mod. Phys. 47, 331 (1975).

[5]P. Bhattachargya, T. -L. Ho, and N. D. Mermin, Phys. Rev. Lett. 39, 1290 (1977). See also M. C. Cross and M. Liu, J. Phys. C 11, 1795 (1978).

[6]V. P. Minneev and G. E. Volovik, Phys. Rev. B 18, 3197 (1978).

[7]T. Tsuneto, T. Ohmi, and T. Fujita, Proceedings of the ULT Hakone Symposium (1977) (unpublished). See also T. Fujita and M. Nakahara, Prog. Theor. Phys. 60, 671 (1978).

[8]P. W. Anderson and G. Toulouse, Phys. Rev. Lett. 38, 508 (1977).

[9]G. E. Volovik and V. P. Minneev, Zh. Eksp. Teor. Fiz. 73, 767 (1977).

[10]T. Fujita, T. Ohmi, and T. Tsuneto, Prog. Theor. Phys. 59, 664 (1978) and 60, 661 (1978). In these references the vortex ring texture is assumed to have cylindrical symmetry, with $\hat{l}$ on the axis turning with it. This is contrary to the types of vortex rings required in the present paper which have axes where $\hat{l} \| \vec{B}$ and can not have cylindrical symmetry.

[11]N. D. Mermin and T. -L. Ho, Phys. Rev. Lett. 36, 594 (1976).

[12]C. -R. Hu, T. E. Ham, and W. M. Saslow, J. Low Temp. Phys. 32, 301 (1978).

[13]N. D. Mermin, in *Quantum Fluids and Solids,* edited by S. B. Trickey, E. D. Adams, and J. W. Dufty (Plenum, New York, 1977), p. 3.

[14]C. -R. Hu, Phys. Rev. B 20, 276 (1979). Earlier references by P. G. de Gennes and D. Rainer, Phys. Lett. A 46, 429 (1974) and by A. L. Fetter, Phys. Rev. B 14, 2801 (1976), preceded this reference in correctly predicting the value of Q_c near T_c, but made an oversimplifying assumption that a planar texture occurs for $Q > Q_c$.

[15]This modified version of A-type coreless vortex texture exists in a background texture with $\chi = 0$ and $\hat{l} \| \hat{z}$ only, and is characterized by an axis γ where $\chi = \pi$, $\hat{l} \| -\hat{z}$, and the quantization condition $(2\pi)^{-1} \int \vec{\nabla} (S_1 + S_2) \cdot d\vec{r} = 2(\Delta n)$. [The separate quantization of S_1 and S_2 as given in Eq. (6) may still be satisfied on some integration paths, but it is no longer a necessary condition.] The corresponding characterization of a modified P-type vortex texture is obvious, but the two types can no longer coexist in a single system. Nevertheless, their kinship with the unmodified version, defined by Eqs. (6), (7), and their accompanying text, may be easily seen, and stressing this kinship is worthwhile, since it provides clues on such questions as why such a vortex-line texture *must* have an axis where $\hat{l} = \mp\hat{z}$ *extending from wall to wall* (but not necessarily a straight line perpendicular to the wall), and how the corresponding ring textures may be constructed. On the other hand, the slight difference in definition here does imply that the $\Delta n = 1$ textures can no longer appear like the Mermin and Ho texture, as is further clarified in the main text.

[16]A. L. Fetter, Phys. Rev. Lett. 40, 1656 (1978) and J. Phys. (Paris) 39, C6-46 (1978). See also H. Kleinert, Y.

R. Lin-Liu, and K. Maki, J. Phys. (Paris) 39, C6-59 (1978), and unpublished.

[17]This double quantization has also been pointed out by Kleinert *et al.* (See the last work cited in Ref. 16.) A very recent report by Kleinert has further elaborated this point.

[18]See C. -R. Hu and W. M. Saslow, Phys. Rev. Lett. 38, 605 (1977); and C. -R. Hu, in *Quantum Fluids and Solids,* edited by S. B. Trickey, E. D. Adams, and J. W. Dufty (Plenum, New York, 1977), p. 105. See also T. L. Ho, *ibid.*, p. 97; H. E. Hall and J. R. Hook, J. Phys. C 10, L91 (1977); D. Lhuillier, J. Phys. Lett. (Paris) 38, 1977 (1977); and J. M. Delrieu, J. Phys. Lett. (Paris) 38, 127 (1977).